Cytometry 13:603–614 (1992)

Eukaryotic DNA Replication is a Topographically Ordered Process[1]

Catherine Humbert and Yves Usson

Equipe de Reconnaissance des Formes et Microscopie Quantitative, Laboratoire TIM3, USR CNRS 00690B, Université Joseph Fourier, BP 53X, 38041 Grenoble Cedex, France

Received for publication July 19, 1991; accepted December 9, 1991

This paper describes the relationship between the BrdUrd replicating pattern of a cell and its localization within the S phase by means of topographical features and DNA content measurement. The present study follows an objective ranking of the BrdUrd patterns obtained from a spectral analysis of the BrdUrd images. The pattern ranking was consistent with the DNA content increase throughout the S phase. Five texture groups were arbitrarily set up for the purpose of multivariate analysis. Nine topographical parameters were computed for each BrdUrd-labelled nucleus. The descriptive quality of these parameters was assessed by means of factorial discriminant analysis. These parameters made it possible to characterize objectively the known pattern distributions of replication sites qualitatively described in the literature. © 1992 Wiley-Liss, Inc.

Key terms: Anti-BrdUrd monoclonal antibodies, fluorescence, topographical parameters, image analysis

There is a body of evidence to support the hypothesis that eukaryotic DNA replication occurs as a nonrandom process in a reproducible temporal order (see 35,40 for review); the best known example is the late replication of the inactive X chromosome of mammalian female (5,21).

The mechanisms responsible for this fixed replication sequence are not known, but factors such as chromatin condensation, DNA functional activity, or intranuclear arrangement may be related to the S phase ordering on the basis of many observations. It is generally conceded that euchromatin replicates early and heterochromatin replicates late. Chromosomal band analysis reveals that early DNA synthesis corresponds to the Giemsa R-band, while late DNA synthesis corresponds to the G-band (14,21). Holmquist suggested that late replication, which gradually appears during developmental process of embryonic cells along with facultative heterochromatinization, may actively determine gene repression (13).

The DNA synthesized in late S might be less important for cell survival than that synthesized in early S. This hypothesis is supported by the data reviewed by Laird et al. (26) indicating that fragile sites in chromosomes of humans, *Drosophila,* and *Microtus* represent regions where DNA replicates late. Furthermore, a number of potentially active genes has been shown to replicate early (12). The relationship between gene activity, intra-nuclear arrangement, and replication timing remains unclear, but alteration of genes, as in translocation, is accompanied by changes in their replication time sequence (21). Iqbal et al. explored the question of "the relationship between the temporal replication of a proto-oncogene and its genomic organization" (18). The existence of a relationship between gene location, involving the nuclear matrix arrangement, and DNA replication has been the subject of a number of biochemical studies (8,19,33,41). However, no definitive answer is available yet, due to the variety of nuclear matrix isolation procedures used (8,38).

To learn more of the DNA replication process as a function of gene activity and location, it is necessary to obtain a better understanding of DNA replication in situ. Inter-nuclear heterogeneity of the replication site distribution has been observed after the replicated DNA was labelled with tritiated thymidine (25,32, 47,48), BrdUrd (2,29,30,31,45), or Biotin-11-UTP

[1]This work was supported by grants from "Pôle Rhône-Alpes Génie Biologique et Médical" and by grant number 6106 from ARC (Association pour la Recherche contre le Cancer).

(3,31). The questions that arose from these observations dealt with the correlation between the occurrence of patterns and the progression of the cells through the S phase, in particular for a possible existence of substages in the S phase, illustrated by these patterns. Following cell synchronization and release, the different replication patterns appear subsequently (3,32, 45,47). The verification of cell synchronization was carried out by parallel measurement of DNA content (propidium iodide staining) using flow cytometry (45), by nuclear area measurement (32), or by comparisons with previous studies (29). Lafontaine et al., working on plant cells, used criteria of volume, regularity of contour, and organization of the chromatin reticulum to order the replicating patterns through the S phase (25). Such approaches made it possible to describe qualitatively the main characteristics of intra-nuclear DNA replication distribution with respect to the beginning or the end of the S phase.

The purpose of this paper is to introduce quantitative data into this field of study; image analysis objectively characterizes the BrdUrd patterns and describes the relationship between a BrdUrd pattern of a cell and its position within the S phase. Simultaneously BrdUrd/PI stained nuclei of normal fibroblastic cells (MRC-5), growing exponentially, were acquired randomly without visual pattern recognition by screening the slide. A cell by cell assessment of BrdUrd and DNA contents and BrdUrd texture features was carried out for each BrdUrd stored image. The present study uses an objective ranking of the BrdUrd patterns obtained from a spectral analysis of the BrdUrd images (43).

MATERIALS AND METHODS

Cell Culture and BrdUrd Incorporation

Normal human fibroblastic MRC5 cells (BioMérieux, Lyon, France) were grown as monolayer cultures on glass slides (Lab-Tek from Miles, Paris, France) at an initial concentration of 5×10^4 cells/ml. Growth medium was BME (Eagle's Basal Medium from BioMérieux, Lyon, France) supplemented with 10% foetal calf serum (Boehringer-Mannheim, Meylan, France), 100 U/ml penicillin, 50 μg/ml streptomycin, 50 μg/ml kanamycin, and 200 mM L-glutamin. The cultures were incubated in a humidified atmosphere of 5% CO_2 at 37°C for 36 h. Exponentially growing cells were incubated for 1 h in fresh growth medium containing 20 μM BrdUrd (Sigma, La Verpillère, France), washed with phosphate-buffered saline (PBS), fixed for 30 min in 70% ethanol at room temperature, and air dried.

Immuno-Cytochemistry

Thermal denaturation in formamide. The slides were immersed in 0.1 M cold HCl for 10 min, and then immersed in 50% formamide in PBS for 30 min at 80°C (9). Thermal denaturation was obtained by immersion in heated water baths and stopped in three successive baths of iced PBS, 0.5% Tween 20 for 15 min.

Indirect immuno-fluorescence staining of BrdUrd. The cells were incubated for 30 min at room temperature with 240 μl of ascites fluid (clone 76-7, mouse anti-BrdUrd monoclonal antibody, a gift from T. Ternynck, Institut Pasteur, Paris) diluted to 1/250 in PBS, 0.5% Tween 20. After two washings in PBS, 0.5% Tween 20 the cells were incubated for 30 min with 240 μl of FITC-conjugated goat anti-mouse immuno-globulins (a gift from Immunotech, Marseille, France) diluted to 1/50 in PBS, 0.5% Tween 20. The cells were then washed two times in PBS, 0.5% Tween 20.

DNA staining. DNA was stained for 30 min at room temperature with 200 μl of propidium iodide (PI) diluted to 50 μg/ml in distilled water, 0.1% sodium citrate. Finally the sample was washed twice with PBS and mounted in glycerol. To ensure PI specificity for DNA, this sample was treated with 300 μl of RNase (500 K-units units/ml RNase A pancreas bovine typeV, Sigma, La Verpillère, France) for 90 min at 37°C and washed twice in distilled water prior to DNA denaturation.

Except for the washing, all steps of staining procedures were carried out between slide and cover-slip to minimize evaporation and the quantity of reagent used. The slides were protected from direct light during the procedures and thereafter stored in the dark.

Fluorescence Image Analysis

A SAMBA^{TM}2005 (System for Analytical Microscopy in Biological Applications; Alcatel-TITN Co., Grenoble, France) fitted with a MATROX MPV/AT (MATROX, Canada) frame grabber and a SIT (Silicon Intensified Targets) camera (LHESA CO., Cergy Pontoise, France) was used for cell image analysis.

Analysis steps. The analysis was divided in two main steps: a) the measurement of the PI and BrdUrd-tagged fluorescence. This was obtained directly by image processing of microscopic fluorescence images; b) the BrdUrd texture pattern analysis: image processing was carried out after an intermediate step of photographing the images.

Measurement of the PI and BrdUrd-tagged fluorescence (a). Acquisition of the fluorescence images (40×, 0.75 NA objective, 0.2 projective). An excitation diaphragm was used to analyze nuclei individually in the center of the microscopic field. BrdUrd labelled nuclei were acquired randomly on the slide without pattern selection. DNA image (PI staining) and BrdUrd image (FITC staining) were digitized into two 512 × 512 superimposable images onto an 8 bit grey scale. The excitation and barrier filter wavelengths used for PI and FITC analysis are listed in Table 1.

Fluorescence measurement. Nuclear segmentation was obtained by image processing of the DNA image. Eleven nuclear parameters were calculated (Table 2) for the DNA fluorescence (six parameters) and BrdUrd-tagged fluorescence (five parameters).

Table 1
Filter Sets Used for Multiple Fluorescence Analysis[a]

	Wavelength (nm)		
	Exciter filter	Dichroic	Barrier filter
FITC	485 ± 20 BP	510 FT	515–565 BP
PI	546 ± 12 BP	580 FT	590 LP

[a]BP, band pass; FT, chromatic beam splitter; LP, longwave pass.

Table 2
List of the 11 Parameters Computed on Nuclear Fluorescence Images[a]

Abbreviation	Parameters
Propidium iodide image	
A	Area
FI-PI	Integrated fluorescence
MF-PI	Mean fluorescence
Stochastic parameters	
SD-PI	Standard deviation of the fluorescence histogram
SKE-PI	Skewness of the fluorescence histogram
KUR-PI	Kurtosis of the fluorescence histogram
BrdUrd image	
FI-BrdU	Integrated fluorescence
MF-BrdU	Mean fluorescence
Stochastic parameters	
SD-BrdU	Standard deviation of the fluorescence histogram
SKE-BrdU	Skewness of the fluorescence histogram
KUR-BrdU	Kurtosis of the fluorescence histogram

[a]Parameters are calculated on the fluorescence histogram for all pixel values within each segmented nucleus.

BrdUrd texture pattern analysis (b). Photography of the BrdUrd images. The SIT generates fuzzy screen images. This fuzziness does not alter the fluorescence measurement (6), but decreases image resolution. For texture pattern analysis, the BrdUrd fluorescence images, were photographed with Tri-XPan 400 Asa film. The films were processed using a standardized development procedure.

Acquisition of the film negative. The negatives of the BrdUrd image photographs were acquired on a macro-photographic bench in transmitted light using a black and white CCD camera (Tokina cp 3000, Tokyo, Japan) connected to the SAMBA™2005. The negatives of BrdUrd images were digitized into 512×512 images onto an 8 bit grey scale.

Texture featuring of the negatives of BrdUrd images. Nuclear segmentation was obtained by image processing of the negatives of BrdUrd images. The description of BrdUrd nuclear distribution was obtained from nine topographical parameters on each nucleus (43), listed in Table 3.

Data analysis. The analysis of the evolution of BrdUrd patterns during the S phase of the cell cycle was carried out on the basis of pattern ranking, PI fluorescence measurement (FI-PI parameter), and multivariate analysis of BrdUrd texture features (factorial discriminant analysis).

A subjective visual ranking of the BrdUrd-labelled nuclei was assessed using spectral analysis followed by clustering techniques (43).

The Spearman rank correlation test was used to verify that the chosen pattern ranking was correlated to the position of cells within the S phase (according to the DNA content). This test was applied to the pattern rank number of nuclei versus their corresponding FI-PI values; 66 nuclei were quantitatively analyzed: 13 nuclei for the first group; 15 nuclei for the second group; 13 nuclei for the third group; 13 nuclei for the fourth, and 12 nuclei for the fifth group.

Five texture groups were arbitrarily set up for the purpose of multivariate analysis. The results of discriminant analysis were expressed by means of factorial discriminant plane representation and confusion matrices. The factorial discriminant plane should be read relative to the modulus and the direction of the parameter projections. It must be also read in term of distances between the different groups: when the distribution of two groups does not differ significantly, their position within the factorial plane are close to each other. Confusion matrices were obtained as follows: each nucleus was reassigned to a texture group as a function of its a posteriori probability obtained by a Bayesian classifier (28). Inter-group mean differences were tested using Student's t test.

RESULTS

Classification of the BrdUrd Labelled Nuclei

The BrdUrd patterns were ordered as described elsewhere (43), taking into account a step by step pattern similarity and spectral analysis (Fig. 1). For the purpose of multivariate analysis, the series of ordered nuclei was divided in five groups which can be described as follows:

First group: the nuclei contain small spots having no relationship with either the nuclear or the nucleolar boundary. The site of nucleoli appears to be devoid of staining. The spot size seems to be constant and the spot number increases as a function of the ordering.

Second group: the large spot number gives an appearance of homogeneous staining. The site of nucleoli is no longer distinguishable.

Third group: this group differs little from the second group, except that some spots are grouped and resembles claws extending from the periphery toward the nuclear center.

Fourth group: the patterns consist of and perinucleolar labelling, with remaining nucleoplasm staining. Nucleoplasmic staining tends to disappear in the last nuclei.

Fifth group: the labelling spots are large, highly fluorescent and well segregated.

Arbitrary limits were drawn between the five groups. However, a feeling of continuous pattern evolution arises from the juxtaposition of the images. The

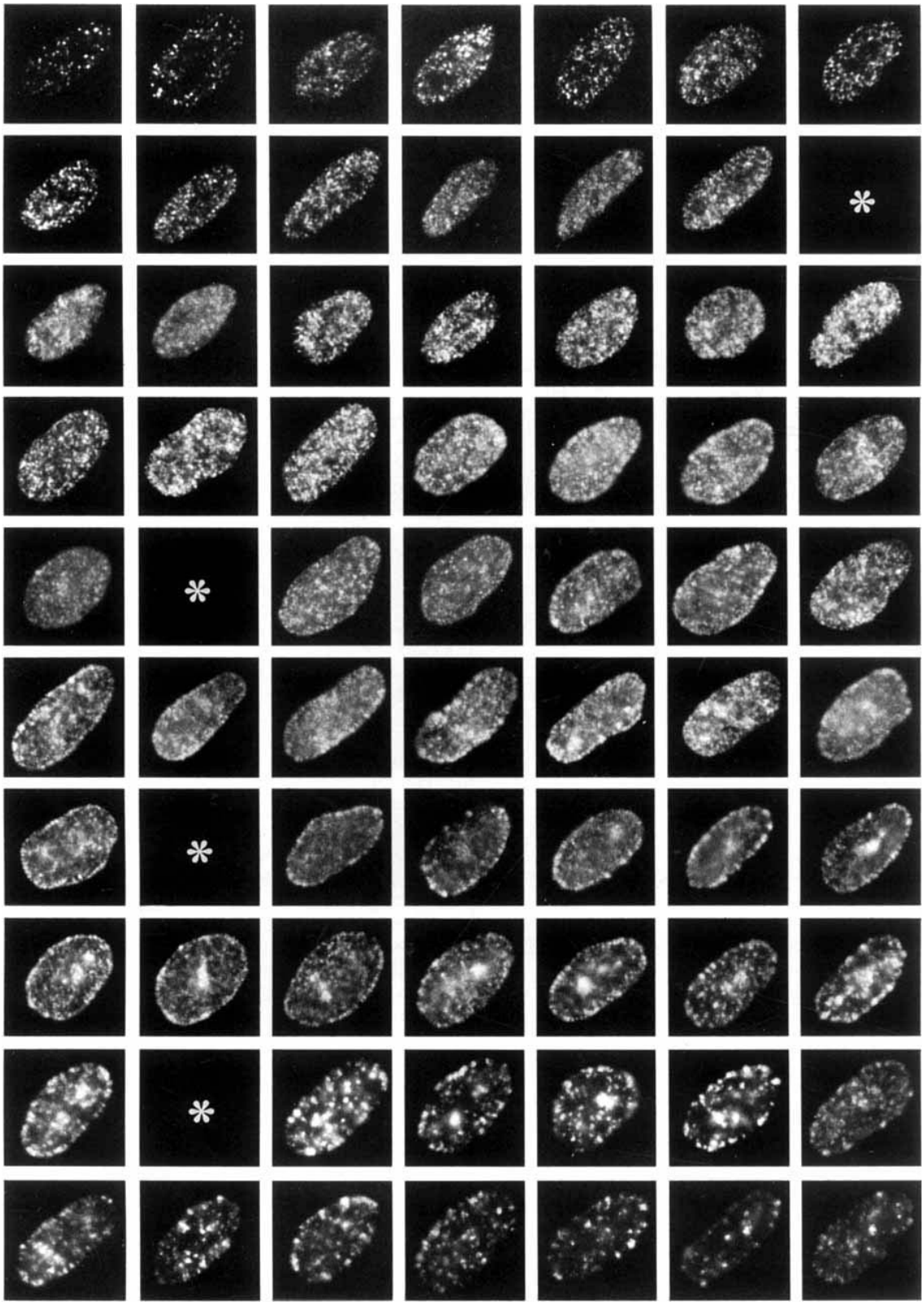

FIG. 1. Pattern ranking of BrdUrd-labelled nuclei. BrdUrd-labelled nuclei were ordered taking into account a stepwise pattern similarity and spectral analysis. The figure must be read from top left to bottom right. Asterisks: arbitrary frontiers between five groups, for the purpose of a texture multiparametric analysis. Note that there is not a great difference between the last nuclei of a group and the first nuclei of the following group. The ranking shows a texture evolution rather than five fixed clusters of patterns. Square side: 15 μm.

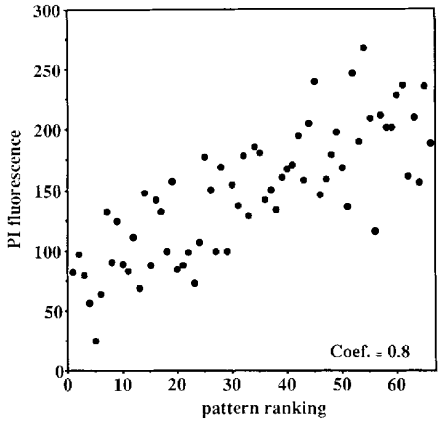

FIG. 2. PI fluorescence measurement (Y axis, arbitrary units) against pattern ranking of BrdUrd-labelled nuclei (X axis, pattern rank numbers). The pattern rank numbers of nuclei (rank) and their corresponding PI fluorescence values (variable) were used in Spearman's rank correlation test. Coef.: rank correlation coefficient. The correlation coefficient significantly differs from 0 at a 0.001 threshold. Number of nuclei: 66.

differences between the last nuclei of one group and the first nuclei of the following group are barely discernable.

Correlation Between the Pattern Rank of a Nucleus and Its DNA Content Measurement

The PI fluorescence values (FI-PI values) of nuclei were plotted against their pattern ranks (Fig. 2). It appears that the pattern rank is linearly related to the PI fluorescence measurement. To statistically confirm that the sequence of nuclei reflects their position within the S phase, the PI fluorescence values of the nuclei and their corresponding rank numbers were submitted to a Spearman rank correlation test. A correlation coefficient of 0.799 was obtained. The correlation coefficient differs significantly from 0 at a 0.001 threshold. This makes it probable that the sequence of nuclei was consistent with the DNA content increase throughout the S phase. Consequently, we may assume that the BrdUrd patterns do not appear randomly during the S phase. However, while the correlation coefficient value is significant, it is not equal to 1 and some PI fluorescence values cover a large range of pattern ranks. In order to evaluate the variability of the propidium iodide (PI) fluorescence intensity, the CV value for PI fluorescence on a population of cells in G0/G1 was calculated. G0/G1 cells were isolated from a population of cells of the same culture doubly stained for PI and BrdUrd by discarding BrdUrd positive cells and G2/M cells. A CV value of 12.6% was obtained for a population of cells in G0/G1.

Texture Analysis of the BrdUrd Patterns

Univariate analysis. In order to characterize the BrdUrd patterns, nine topographical parameters (listed in Table 3) were computed on each labelled nucleus. The mean values per texture group (as defined in Fig. 1) of the topographical parameters (listed in Table 3) are represented in Figure 3. For comparison, the mean values per texture group of the stochastic parameters (listed in Table 2) are also shown in the figure. To help in the interpretation of this figure, the mean values of the topographical parameters were compared between all possible pairs of texture groups, by means of a Student's t test (Table 4).

Table 3
List of the Nine Topographical Parameters Computed on BrdUrd Nuclear Images[a]

Abbreviation	Parameters
High fluorescence class	
A%HF	Relative area
MDHF	Mean distance to the nuclear border
SDHF	Standard deviation of distances from the nuclear border
Middle fluorescence class	
A%MF	Relative area
MDMF	Mean distance to the nuclear border
SDMF	Standard deviation of distances from the nuclear border
Low fluorescence class	
A%LF	Relative area
MDLF	Mean distance to the nuclear border
SDLF	Standard deviation of distances from the nuclear border

[a]The principle of computation is described elsewhere (see 43).

The texture groups can be described according to the topographical texture parameters (Fig. 3). For example, the first group can be described according to Figure 3 as follows: there are almost as many sites with intense staining as sites without (relative areas, first row). The staining site distribution is not spread over the whole nuclear area (low value of the distance from edge standard deviation of high fluorescence class, SDHF, third row, first column) and is rather peripheral (low mean distance from edge of the same class, MDHF, second row, first column). The sites devoid of staining display a more widespread distribution (high value of the distance from edge standard deviation of the low fluorescence class, SDLF value, third row, third column) with a prefered centered localization (high mean distance from edge of the same class, MDLF value, second row, third column).

The comparison of the mean values of topographical parameters (Table 4) makes it possible to investigate the contribution of the parameters to distinguish the different texture groups. It appears that the mean values of four parameters (A%HF, A%LF, MDLF, SDLF) are significantly different between each pair of neighboring groups, except between the second and third group. The mean values of other parameters are significantly different only between one pair of groups (i.e., MDHF for 1 vs. 2; SDHF for 3 vs. 4). The first group (beginning of the S phase) and the fifth group

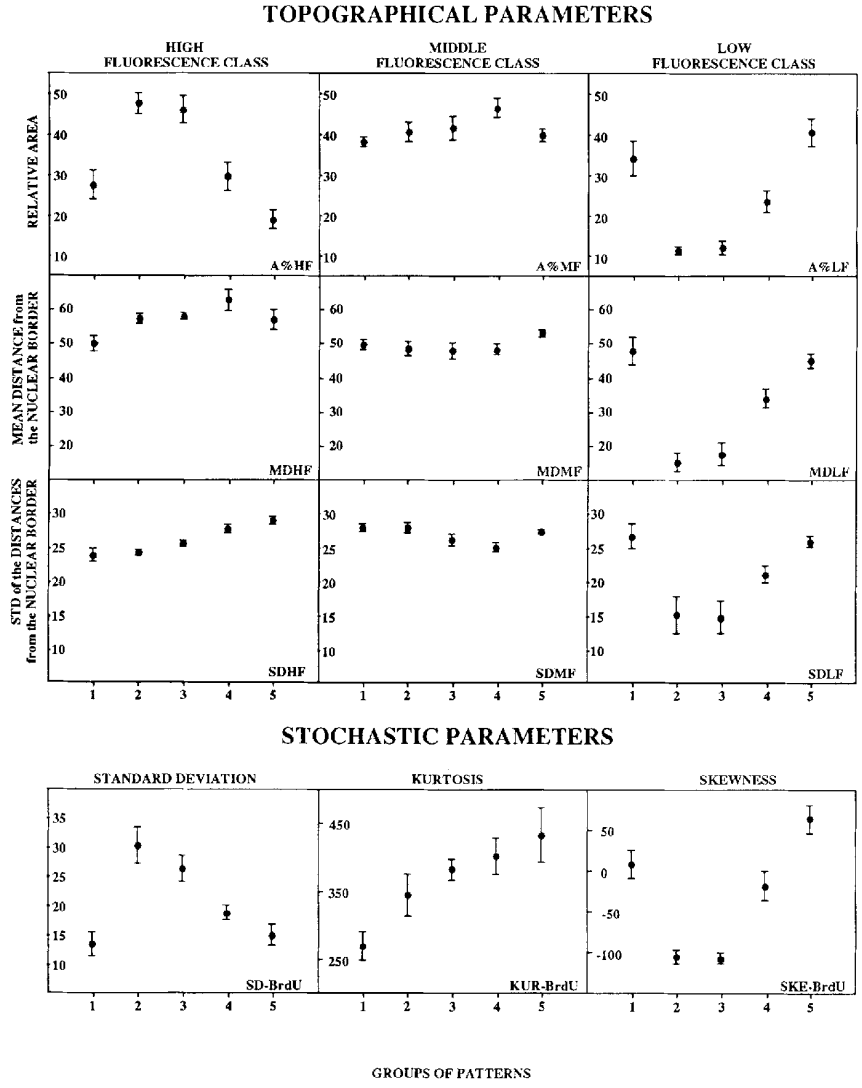

FIG. 3. Mean values of topographical and stochastic parameters (Y axis) of each texture group (X axis, group numbers). Bars: standard errors on the mean (standard deviation/n). The names of the parameters are indicated to the left of panel lines, the fluorescence class at the top of columns. The names of stochastic parameters are indicated at the top of panels. The name abbreviations are written at the right bottom of panels.

(end of the S phase) show resemblances for eight out of nine topographical parameters (no significant differences). These two groups differ only for distance from the edge standard deviation of the high fluorescence class (SDHF). Figure 3 shows that SDHF mean value is lower for the first group than for the fifth, translating the observation that the staining sites are excluded from the center of nuclei in the first group and not in the fifth group.

Some parameters display direct or inverse correlation. Table 5 gives the correlation coefficient for the parameter pairs. There is a correlation between topographical parameters and stochastic parameters (i.e., the correlation for A%LF and SKE-BrdU, skewness of the BrdUrd fluorescence histogram, is 0.85; the correlation of SD-BrdU, standard deviation of the BrdUrd fluorescence histogram, and A%HF is 0.71).

Factorial discriminant analysis. To summerize the differences or resemblances between the five texture groups taking into account all the topographical parameters simultaneously, we used a factorial discriminant analysis. Figure 4 represents the projection of the texture groups (95% tolerance means) on the first discriminant plane as well as the respective contribution of parameters in describing the groups. The analysis of the factorial plane shows the following trends

Table 4
Statistical Comparison of Means of Texture Groups (Student's t Test) for the Nine Topographical Parameters[a]

	A%HF	MDHF	SDHF	A%MF	MDMF	SDMF	A%LF	MDLF	SDLF
1 vs. 2	+ + +	+	—	—	—	—	+ + +	+ + +	+ +
2 vs. 3	—	—	—	—	—	—	—	—	—
3 vs. 4	+ +	—	+ +	—	—	—	+ +	+ +	+
4 vs. 5	+	—	—	+	+	+ +	+ + +	+ +	+ +
1 vs. 3	+ + +	+ +	—	—	—	—	+ + +	+ + +	+ + +
1 vs. 4	—	+ +	+ +	+ +	—	+ +	+	+ +	+
1 vs. 5	—	—	+ + +	—	—	—	—	—	—
2 vs. 4	+ + +	—	+ + +	—	—	+ +	+ + +	+ + +	—
2 vs. 5	+ + +	—	+ + +	—	—	—	+ + +	+ + +	+ +
3 vs. 5	+ + +	—	+ + +	—	—	—	+ + +	+ + +	+ + +

[a]Column entries: topographical parameters. Row entries: pairs of compared texture groups (e.g., 1 vs. 2: first group versus second group). Significance levels: + + +, means significantly different with $p < 0.001$; + +, means significantly different with $P < 0.01$; +, means significantly different with $P < 0.05$; —, means not significantly different $P \geq 0.05$. The Table is divided in two parts: the upper panel concerns adjacent groups with respect to Figure 1 and the lower panel concerns the remaining combinations.

Table 5
Linear Correlation Coefficients[a]

	SD-BrdU	SKE-BrdU	KUR-BrdU	A%HF	MDHF	SDHF	A%MF	MDMF	SDMF	A%LF	MDLF	SDLF
SD-BrdU	1.000											
SKE-BrdU	−0.506	1.000										
KUR-BrdU	−0.285	0.226	1.000									
A%HF	**0.713**	**−0.711**	−0.346	1.000								
MDHF	0.284	−0.082	0.146	0.085	1.000							
SDHF	−0.224	0.217	0.338	−0.257	0.329	1.000						
A%MF	−0.091	−0.226	0.302	−0.313	0.176	0.212	1.000					
MDMF	−0.283	0.072	0.067	−0.363	−0.241	0.162	0.334	1.000				
SDMF	0.017	−0.008	−0.169	−0.074	−0.331	−0.196	−0.065	0.688	1.000			
A%LF	−0.687	**0.852**	0.191	**−0.859**	−0.179	0.149	−0.217	0.191	0.111	1.000		
MDLF	**−0.716**	**0.714**	0.009	**−0.731**	−0.320	0.138	−0.069	0.190	0.091	**0.791**	1.000	
SDLF	−0.620	0.530	0.014	−0.574	−0.261	0.114	0.010	0.286	0.156	0.588	**0.886**	1.000

[a]The correlation coefficients were calculated on the merged groups. The correlation coefficients greater than [0.7] are in bold type.

(Fig. 4): The second and third group display staining over the whole nuclear area when compared to the other groups. The relative area of high fluorescence class (A%HF) contributes to the discrimination between group two, three, and the others.

The stained spots are more distant from each other in the fourth and fifth group (staining concentrated in large spots with a heterogeneous localization) than in the first. Thus, the standard deviation of the distances from the nuclear border for high fluorescence class (SDHF) contributes largely to the discrimination between the first group and the fourth and fifth.

The fourth group differs from the fifth according to the middle fluorescence class. The remaining nucleoplasmic staining of nuclei of the fourth group adds to the relative area of middle fluorescence class, and the distribution of this fluorescence class is more collected for the fourth than for the fifth group. The projections of SDMF and A%MF illustrate how these parameters contribute in discriminating the fourth group from the fifth. The fifth group shows more sites without staining than fourth group and it differs from fourth due to its low fluorescence class parameters as well.

For illustration, Table 6 shows the rate of well classified cells for each group after a stepwise discriminant analysis. Using a Bayesian classifier, the best classification rate is 83%. However, the number of the learning set must be increased to insure a robust classifier.

Although it is easy and informative to describe the general features of texture groups, there is actually a texture evolution rather than five fixed clusters of patterns. This leads to intra-group deviations, as illustrated in Figure 5 (upper panel) by the evolution of the most discriminant parameter (A%HF) with respect to the pattern ranking of Figure 1. Some groups display large intra-group deviations (for example the first group) and some are more homogeneous according to this parameter (fifth group).

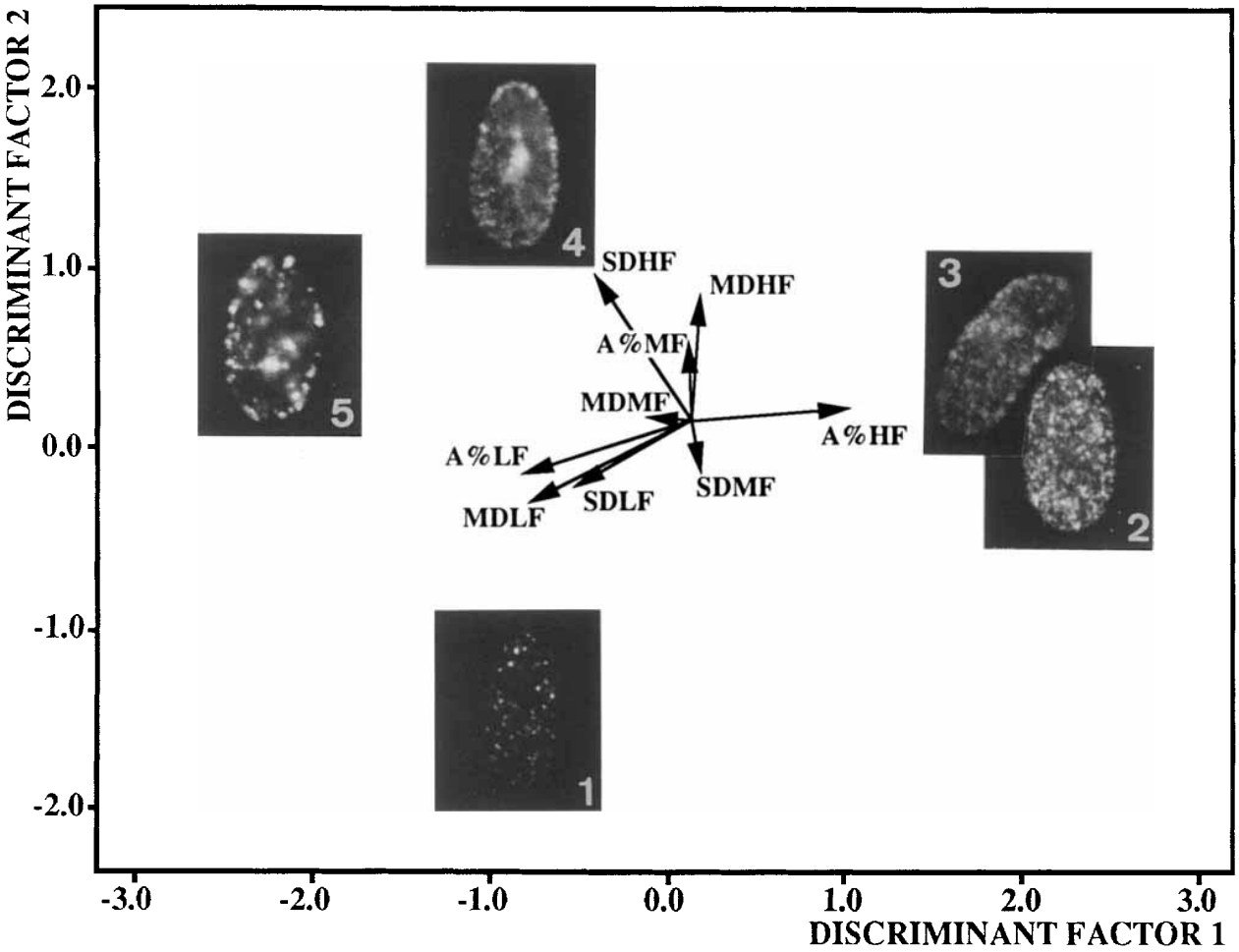

FIG. 4. Factorial discriminant analysis of the five texture groups using the topographical parameters (nine parameters listed in Table 3). The axes represent a linear combination of parameters (discriminant factor). The projection on the axes of each parameter (lines drawing from the center of figures) gives the contribution of parameters to the discriminant factors. Characteristic BrdUrd nuclear images indicate the position of the 95% tolerance means of each texture group. Number of nuclei: 13 for the first group, 15 for the second, 13 for the third, 13 for the fourth, and 12 for the fifth. Long side of images: 25 μm.

Relationship Between BrdUrd Tagged Fluorescence Measurement (BrdUrd Content) and BrdUrd Texture Patterns

BrdUrd content versus pattern ranking. Figure 5, lower panel, shows that the higher BrdUrd-tagged fluorescence values (high BrdUrd content) occur when the nuclei display the patterns of the second and the third group. In these groups the difference in the BrdUrd nuclear content is the largest. This panel shows the differences in replication activity intensity (BrdUrd content) per replication activity type (BrdUrd spatial distribution, pattern groups).

Figure 6 shows the scattergram representation of BrdUrd-tagged fluorescence (BrdUrd content) versus PI fluorescence (DNA content). The pattern groups are plotted in this figure. There is a large variability in BrdUrd content (replication activity intensity) for cells with the same DNA content, as well as for cells with similar BrdUrd spatial distributions (replication activity type).

BrdUrd content versus a topographical parameter. The evolution of BrdUrd tagged fluorescence of nuclei along with pattern ranking is similar to the evolution of the relative area of high fluorescence class (Fig. 5, compare the two panels).

DISCUSSION

Classification of the BrdUrd Labelled Cells

Subjective visual ranking of the BrdUrd-labelled nuclei was assessed by a spectral analysis of the stored

Table 6
Confusion Matrix[a]

	First	Second	Third	Fourth	Fifth	CR%
First	**10**	0	2	0	1	
Second	0	**14**	1	0	0	
Third	0	4	**8**	1	0	83.0
Fourth	0	0	1	**12**	0	
Fifth	0	0	0	1	**11**	

[a]The confusion matrix was obtained by classification of BrdUrd-labelled nuclei after the seventh step of a stepwise discriminant analysis using nine topographical variables. The seven variables were MDLF, SDHF, A%LF, SDMF, SDLF, MDMF, and MDHF. The two remaining variables (A%MF and A%HF) did not significantly improve the good classification rate. In such a matrix, rows are the groups of origin of the nuclei and columns are the groups where the nuclei were assigned by a Bayesian classifier. Bold faced numbers indicate the number of well classified BrdUrd-labelled nuclei. CR%, good classification rate.

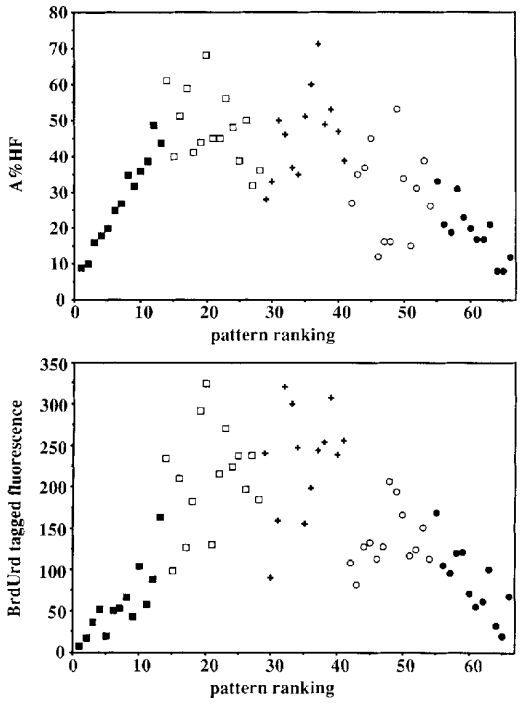

FIG. 5. Scattergram of the relative area of high fluorescence class (A%HF, upper panel) and BrdUrd-tagged fluorescence (arbitrary units) versus the pattern ranking (according to Fig. 1). First group: ■; second group: □; third group: +; fourth group: ○; fifth group: ●.

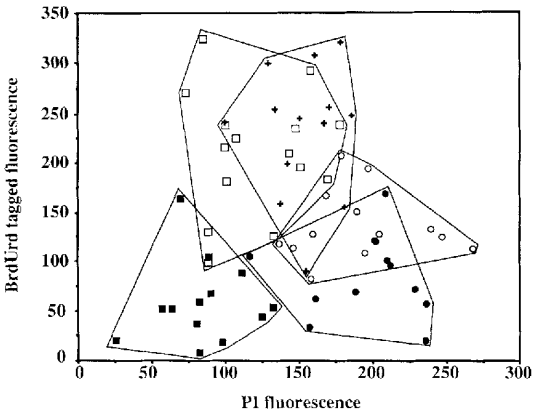

FIG. 6. Scattergram of the BrdUrd-tagged fluorescence measurement versus PI fluorescence measurement (arbitrary units) for the BrdUrd-labelled nuclei. Pattern groups are plotted according to the classification in Figure 1. Each group is surrounded by its convex hull. First group: ■; second group: □; third group: +; fourth group: ○; fifth group: ●.

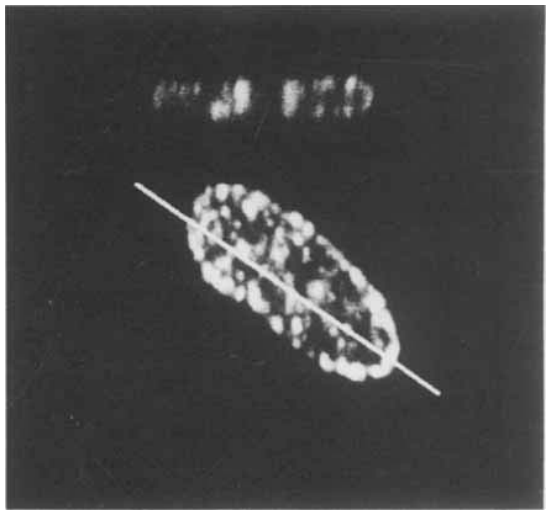

FIG. 7. Laserscan confocal optical section, parallel to the optical axis. One nucleus and its section line are represented (bottom), as well as the resulting optical section (top). Note the flattened shape of the MRC-5 nucleus. Section width: 3 μm.

images followed by clustering techniques (43). We stress that a classification based on visual screening of the slide lacks the notion of dynamic changes in pattern (as shown in Fig. 1) and leads to the notion of static clusters of patterns. When the most typical nuclei from each cluster are chosen, the continuum is no longer evident, each of these nuclei being maximally different from the others (compare the impression resulting from a comparison of Fig. 1 with Fig. 4 where only characteristic images were selected). Subjective recognition may introduce errors because certain images of nuclear organization may be more attractive or typical for the human observer, and these images may therefore be chosen more frequently (37). Moreover, we observed that with storage and juxtaposition of images, nuclei from different microscopic fields, which seemed similar, were in fact very different, and vice versa. This could explain why some authors indicate fractions of unclassified nuclei when making S phase partitions (32), or why authors reported that two (25),

three (31), or five (45) texture groups could be distinguished during the S phase. Therefore, the existence of well separated sub-phases during S phase should be postulated with caution, and some authors have prefered the concept of overlapping groups (45).

The partition into groups was necessary for the purpose of multiparametric analysis, but the arbitrarily drawn frontiers between groups does not imply the existence of actual limits between sub-phases in the S phase.

Correlation Between the BrdUrd Pattern Ranking and the DNA Content of Cells

We statistically tested whether our pattern ranking was consistent with an increase in DNA content throughout the S phase (Fig. 2). Thus, with respect to a simultaneous estimation of the progression of cells within the S phase (BrdUrd vs. PI fluorescence measurement from double stained nuclei), we may assume that the occurrence of various BrdUrd patterns reflects a specific topographical arrangement of the DNA synthesis sites during the S phase rather than a random event.

While the correlation coefficient was significant and suggested that the BrdUrd patterns are correlated with the progression of cells within the S phase at the cell population level, we observed that overlapping between different texture types occurs with respect to the DNA content (Fig. 6). This may be due to immunocytochemistry artefacts and/or fluorescence measurement errors. The PI CV value of 12.6% obtained for a population of G0/G1 cells is not negligible and could partly account for the group overlappings. However, such group overlappings can be inferred from other studies, where the landmark was not the DNA content measurement, but cell synchronization (31), or nuclear area measurement (45). Accordingly, overlapping may be due to factors other than fluorescence measurement errors.

These factors may also account for the variations in the BrdUrd content between cells with the same DNA content and the same BrdUrd patterns. Figure 6 illustrates how much the differences in replication activity intensity (BrdUrd content), and replication activity types (BrdUrd spatial distribution) may contribute to the large variability in BrdUrd content observed for cells with the same DNA content. Arguments against the problem of immuno-cytochemistry artefacts can be deduced from studies on PCNA, the auxiliary protein of the mammalian DNA polymerase ∂, whose intra-nuclear distribution is very similar to BrdUrd distribution. Some authors reported that the transition between different PCNA patterns does not take place simultaneously in all cells of a synchronized population (7). Double PCNA/DNA quantification led to scattergrams showing large variations of PCNA content for cells with the same DNA content (24), which were similar to those obtained from BrdUrd/DNA quantification (15,42). Immunocytochemistry steps are very different between PCNA and BrdUrd procedures (BrdUrd immuno-revelation needs BrdUrd incorporation and DNA denaturation; PCNA immuno-revelation needs neither PCNA incorporation nor DNA denaturation). Taking into account the similarity between BrdUrd and PCNA quantification results (see above) and the differences between the immunocytochemistry procedures, it is unlikely that only immunocytochemistry artefacts, such as imperfect BrdUrd incorporation or incomplete DNA denaturation, can account for BrdUrd content variations for a given DNA content, or for BrdUrd pattern group overlappings.

We should consider whether speed of S phase traverse, or the temporal order of the DNA replication, are responsible for the BrdUrd content (replication activity intensity) variations and pattern (replication activity type) overlappings. Although S phase is considered to be of constant duration, its length can vary in vivo between different development stages of the same species (44), and in vitro it depends on the medium tonicity (34). Gezer et al. (11) found that the differentiation of HL-60 cells in response to retinoic acid slows down the cell cycle as a result of a prolongation of both the S and the G1 phase of the cell cycle. Skehan reviewed articles on the regulation of the generation time by changes in the duration of S phase (39). One wonders whether small differences may also occur between cells of the same line and the same culture and thus lead to the variations in BrdUrd content for cells with the same DNA content. In addition to these variations, flexibility of temporal order of the DNA replication may occur within the S phase. DNA replication does not progress continuously during the S phase (22,23), and on the chromosome, but also proceeds by a scattered firing of replicon clusters. It may be possible that the firing of particular replicons is not exactly synchronized in a population of cells. The groups of patterns 2 and 3 have scattered small spots, homogeneously distributed in the nucleus, and show both the highest content and greatest variations in BrdUrd content. This suggests that a large portion of DNA is synthesized in those nuclei (high BrdUrd content) and may be with a flexible program (high variations of BrdUrd content). Additional arguments for the flexibility of temporal order of the DNA replication come from the increasing number of reports on the coordination of DNA replication with transcription (1,17,27). Prescott (36) thus concluded that "the ordered structure of S phase is flexible at least to the extent that DNA transcription is a flexible regulated process." DNA replication can be assumed to be an ordered process, in the sense that some main events take place before others, but the events may not be that rigorously controlled by time or DNA content at the replicon level.

Texture analysis of the BrdUrd labelled nuclei

Nuclear shape (confocal analysis). It was necessary to verify that BrdUrd pattern recognition and classification did not depend on the focal plane chosen,

as stressed by Mazzoti (29) for spherical nuclei. The confocal optical sections obtained from the MRC-5 nuclei (Fig. 7) confirm that two-dimensional images of these nuclei can be considered to be independent of the focal plane, because of their flattened shape and the field depth (1.43 μm) of the objective lens (40 × /0.75).

Picturing power of topographical parameters. Because they make it possible to codify visual experience, the topographical parameters are easy to interpret. One can predict which parameter should be used in order to discriminate one pattern from another. For example, the standard deviation of the distances from the nuclear border (SDHF) is a useful parameter to discriminate the pattern group 1 from 5. This is an old dream of synthesizing the image of a nucleus from its computer description. The topographical parameters constitute a step forward in this endeavour.

Correlation between topographical and stochastic parameters. The use of topographical parameters combined with the stochastic parameters provides a means of interpreting the latter which are otherwise difficult to understand. The skewness of the BrdUrd fluorescence histogram (SKE-BrdU) is correlated at 85% with A%LF and inversely correlated at 71.1% with A%HF. When fluorescence classes are equally represented, there is no skewness which only appears when one fluorescence class increases with respect to the others. The standard deviation of the BrdUrd fluorescence histogram (SD-BrdU) is correlated with A%HF parameter and shows the highest values for the second and third group. This is because increased fluorescence leads to a larger halo surrounding each spot, making the fluorescence histogram bimodal for each nucleus. Thus, such parameters may be useful for discriminating between groups but must be used carefully to describe a texture, because nuclei having a large range of intensities can have a lower SD-value than nuclei having two narrow but distant modes of intensities.

BrdUrd content versus topographical parameters. Because the fluorescence intensities and nuclear shape are not used in the mathematical definition of the topographical parameters, the correlation observed between the BrdUrd content (BrdUrd tagged fluorescence) and the relative area of high fluorescence class (A%HF) (Fig. 5) has a biological significance (when a site is stained it seems to be of similar intensity from one nucleus to another) and is not a calculation artefact. Thus, it is possible to interpret the values of A%HF and A%LF in terms of sites of BrdUrd incorporation and sites without, A%MF contributing to the incertainty.

Biological Relevance of the Replication Site Distribution

Typical figures. The main changes from the beginning to the end of the S phase concern the size of spots (small at the beginning, large at the end), the spot number (maximum in the middle), location close to the nuclear, and nucleolar boundaries (absent at the beginning and in the middle, perinuclear and perinucleolar thereafter, and perinuclear at the end). These results are in agreement with previous findings (20,25,45,47).

Early replication. Since the cells were acquired randomly and the cell proportions were respected, it may be assumed that some cells did not spend the entire labelling hour in the S phase, and therefore the first images of the ranking reflect an incubation time gradient. The increasing spot number and the constant size of spots observed in these cells indicated that early replication occurs asynchronously. Here we concur with Vogel et al. (46).

Late replication. Two main characteristics of the late replication patterns are the perinuclear and perinucleolar labelling and the large spot size. This suggests that the late replication involves heterochromatin, as it is generally accepted (20,35). The fact that BrdUrd spots appear condensed is not surprising since replication could occur on condensed material, such as mitotic figures (16), and in vitro even across the nucleosome without histone displacement (4). In fact, the observed patterns do not exclude other possibilities: the larger spot size could also reflect an increased rate of DNA synthesis in late S (5), a larger portion of AT-rich sequences (13), or simply indicate a large quantity of DNA. Furthermore, some questions remain. Does the staining annulus actually result from constitutive heterochromatin replication, or is it the result of the replication of DNA in prophase condensation phase (10)?

Topographical parameters provide quantitative description of the BrdUrd patterns during the S phase (topography, DNA, and BrdUrd content measurement), instead of visual and subjective description. Applied to the studies of double BrdUrd/DNA texture analysis (20), these topographical parameters should contribute to improving the understanding of replication with respect to the chromatin condensation state. It would also be of fundamental interest to combine techniques of BrdUrd labelling and in situ hybridization to localize a sequence, when it is replicated, as a means of S phase compartmentalization studies.

ACKNOWLEDGMENTS

The authors wish to thank Dr. Thérèse Terninck for providing the BrdUrd monoclonal antibody, Dr. Victoria von Hagen for her advice editing of the manuscript, Dr. Michèle Brugal for documental assistance, and Mrs. Yolande Bouvat for photographic technical assistance.

LITERATURE CITED

1. Almouzni G, Méchali M, Wolffe AP: Competition between transcription complex assembly and chromatin assembly on replicating DNA. EMBO J 9:573–582, 1990.
2. Arndt-Jovin DJ, Robert-Nicoud M, Jovin TM: Probing DNA structure and function with a multi-wavelength fluorescence confocal laser microscope. J Microsc 157:61–72, 1990.
3. Banfalvi G, Wiegant J, Sarkar N, van Duijn P: Immunofluores-

cent visualization of DNA replication sites within nuclei of Chinese hamster ovary cells. Histochemistry 93:81–86, 1989.
4. Bonne-Andrea C, Wong ML, Alberts BM: In vitro replication through nucleosomes without histone displacement. Nature 343: 719–726, 1990.
5. Camargo M, Cervenka J: Patterns of DNA replication of human chromosomes. II. Replication map and replication model. Am J Hum Genet 34:757–780, 1982.
6. Camus E, Santisteban Otegui MS, Monet JD, Brugal G: Fluorescence quantitation in cytology by video-microfluorometry. Inov Tech Biol Med 11:96–106, 1990.
7. Celis JE, Celis A: Cell cycle-dependent variations in distribution of the nuclear protein cyclin proliferating cell nuclear antigen in cultured cells: Subdivision of S phase. Proc Natl Acad Sci USA 82:3262–3266, 1985.
8. Djondjurov L, Ivanova E, Markov D, Bardarov S, Sachsenmaier W: Is the nuclear matrix the site of DNA replication in eukaryotic cells? Exp Cell Res 164:79–96, 1986.
9. Dolbeare F, Beisker W, Pallavicini MG, Vanderlaan M, Gray JW: Cytochemistry for bromodeoxyuridine/DNA analysis: Stoichiometry and sensitivity. Cytometry 6:521–530, 1985.
10. El-Alfy M, Leblond CP: Visualization of chromosome assembly during the S and G2 stages of the cycle and chromosome disassembly during the G1 stage in semithin sections of mouse duodenal crypt cells and other cells. Am J Anat 183:45–56, 1988.
11. Gezer S, Yasin Z, Imren S, Freeman J, Black A, Raza A: Changes observed in the growth fraction, labeling index, duration of S phase, and total cell cycle times of HL-60 cells as they undergo differentiation in response to retinoic acid. Cancer Res 48:5989–5994, 1988.
12. Goldman MA, Holmquist GP, Gray MC, Caston LA, Nag A: Replication timing of genes and middle repetitive sequences. Science 224:686–692, 1984.
13. Holmquist GP: Role of replication time in the control of tissue-specific gene expression. Am J Hum Genet 40:151–173, 1987.
14. Holmquist G, Gray M, Porter T, Jordan J: Characterization of Giemsa dark- and light-band DNA. Cell 31:121–129, 1982.
15. Humbert C, Giroud F, Brugal G: Detection of S cells and evaluation of DNA denaturation protocols by image cytometry of fluorescent BrdUrd labelling. Cytometry 11:481–489, 1990.
16. Hutchison C, Kill I: Changes in the nuclear distribution of DNA polymerase alpha and PCNA/cyclin during the progress of the cell cycle, in a cell-free extract of Xenopus eggs. J Cell Sci 93:605–613, 1989.
17. Iguchi-Ariga SMM, Ariga H: Concerted mechanism of DNA replication and transcription. Cell Struct Funct 14:649–651, 1989.
18. Iqbal MA, Chinsky J, Didamo V, Schildkraut CL: Replication of proto-oncogenes early during the S phase in mammalian cell lines. Nucleic Acids Res 15:87–103, 1987.
19. Jackson DA, McCready SJ, Cook PR: Replication and transcription depend on attachment of DNA to the nuclear cage. J Cell Sci Suppl 1:59–79, 1984.
20. Jovin TM, Arndt-Jovin DJ: Luminescence digital imaging microscopy. Annu Rev Biophys Biophys Chem 18:271–308, 1989.
21. Karube T, Watanabe S: Analysis of the chromosomal DNA replication pattern using the bromodeoxyuridine labeling method. Cancer Res 48:219–222, 1988.
22. Klevecz RR, Kapp LN: Intermittent DNA synthesis and periodic expression of enzyme activity in the cell cycle of WI-38. J Cell Biol 58:564–573, 1973.
23. Klevecz RR, Keniston BA: The temporal structure of S phase. Cell 5:195–203, 1975.
24. Kurki P, Ogata K, Tan EM: Monoclonal antibodies to proliferating cell nuclear antigen (PCNA)/cyclin as probes for proliferating cells by immunofluorescence microscopy and flow cytometry. J Immunol Methods 109:49–59, 1988.
25. Lafontaine JG, Lord A: An ultrastructural and radio-autographic study of the evolution of the interphase nucleus in plant meristematic cells (*allium porrum*). J Cell Sci 14:263–287, 1974.
26. Laird C, Jaffe E, Karpen G, Lamb M, Nelson R: Fragile sites in human chromosomes as regions of late-replicating DNA. TIG 3: 274–281, 1987.
27. Laskey RA, Fairman MP, Blow JJ: S phase of the cell cycle. Science 246:609–614, 1989.
28. Manly BFJ: Multivariate Statistical Methods: A Primer. Chapman and Hall, London, 1986, pp 86–99.
29. Mazzoti G, Rizzoli R, Galanzi A, Papa S, Vitale M, Falconi M, Neri LM, Zini N, Maraldi NM: High-resolution detection of newly synthesized DNA by anti-bromodeoxyuridine antibodies identifies specific chromatin domains. J Histochem Cytochem 38:13–22, 1990.
30. Nakamura H, Morita T, Sato C: Structural organizations of replicon domains during DNA synthetic phase in the mammalian nucleus. Exp Cell Res 165:291–297, 1986.
31. Nakayasu H, Berezney R: Mapping replicational sites in the eukaryotic cell nucleus. J Cell Biol 108:1–11, 1989.
32. Nicolini C, Belmont AS, Martelli A: Critical nuclear DNA size and distribution associated with S phase initiation: Peripheral location of initiation and termination sites. Cell Biophys 8:103–117, 1986.
33. Pardoll DM, Vogelstein B, Coffey DS: A fixed site of DNA replication in eukaryotic cells. Cell 19:527–536, 1980.
34. Pellicciari C, Mazzini G, Fuhrman Conti AM, De Grada L, Manfredi Romanini MG: Effect of hypertonic medium on human cell growth: III. Changes in cell kinetics of EUE cells. Cell Biol Int Rep 13:345–356, 1989.
35. Prescott DM: Initiation of DNA synthesis and progression through the S period. In: Cell Growth, Nicolini C (ed). Plenum Press, New York, 1982, pp 355–364.
36. Prescott DM: Cell reproduction. Int Rev Cytol 100:93–128, 1987.
37. Russ JC: Lessons from human vision. In: Computer-Assisted Microscopy: The Measurement and Analysis of Images. Plenum Press, New York, 1990, pp 439–450.
38. Rzeszowska-Wolny J, Razin S, Puvion E, Moreau J, Scherrer K: Isolation and characterization of stable nuclear matrix preparations and associated DNA from avian erythroblasts. Biol Cell 64:13–22, 1988.
39. Skehan P: Control models of cell cycle transit, exit, and arrest. Biochem. Cell Biol 66:467–477, 1988.
40. Smith JA: The cell cycle and related concepts in cell proliferation. J Pathol 136:149–166, 1982.
41. Smith HC, Puvion E, Buchholtz LA, Berezney R: Spatial distribution of DNA loop attachment and replicational sites in the nuclear matrix. J Cell Biol 99:1794–1802, 1984.
42. Stevenson AP, Crissman HA, Stewart CC: Macrophage-induced cytostasis: kinetic analysis of bromodeoxyuridine-pulsed cells. Cytometry 6:578–583, 1985.
43. Usson Y, Humbert C: Methods for topographical analysis of intranuclear BrdUrd-tagged fluorescence. CYTO 13:595–603, 1992.
44. Usson Y, Saxod R: Schwann cell proliferation in the sciatic nerve of hypothyroid chick embryos studied by autoradiography and image analysis. J Neurocytol 17:639–648, 1988.
45. Van Dierendonck JH, Keyzer R, Van de Veld CJH, Cornelisse CJ: Subdivision of S-phase by analysis of nuclear 5-bromodeoxyuridine staining patterns. Cytometry 10:143–150, 1989.
46. Vogel W, Autenrieth M, Mehnert K: Analysis of chromosome replication by a BrdUrd antibody technique. Chromosoma 98:335–341, 1989.
47. Williams CA, Ockey CH: Distribution of DNA replicator sites in mammalian nuclei after different methods of cell synchronization. Exp Cell Res 63:365–372, 1970.
48. Wise GE, Prescott DM: Initiation and continuation of DNA replication are not associated with the nuclear envelope in mammalian cells. Proc Natl Acad Sci USA 70:714–717, 1973.